Absolute cross sections for $2s$-$2p$ excitation of N^{4+} by electron impact

D. Gregory* and G. H. Dunn†

Joint Institute for Laboratory Astrophysics, University of Colorado and National Bureau of Standards, Boulder, Colorado 80309

R. A. Phaneuf and D. H. Crandall

Oak Ridge National Laboratory, Oak Ridge, Tennessee 37830

Absolute cross sections have been measured for $1s^2 2s\,^2S_{1/2}$-$1s^2 2p\,^2P_{1/2,3/2}$ excitation of lithiumlike N^{4+} by electron impact. For this process, which has a threshold at 10 eV, relative cross sections measured at several energies between 4 and 52 eV were normalized to a single absolute measurement taken at 15.5 eV. Similar data for Li-like C^{3+} have been previously reported and are presented for comparison. In both cases, allowing for the experimental electron energy spread, the measurements agree within experimental uncertainties with published Coulomb-Born and close-coupling calculations over the entire experimental energy range. Rate coefficients as a function of electron temperature are also presented for the N^{4+} transition.

I. INTRODUCTION

The excitation of multiply charged ions by electron impact is an important fundamental atomic collision process with particular significance to the diagnostics and modeling of high-temperature plasmas.[1] Relatively small concentrations of partially stripped impurity ions in magnetically confined thermonuclear fusion plasmas can seriously inhibit plasma heating and initiate instabilities.[2] Line radiation from impurity ions is the most serious energy loss from current tokamaks.[3,4] In such cases, accurate knowledge of specific excitation cross sections or rate coefficients is required in order to assess impurity concentrations. In high-temperature plasmas, both produced in the laboratory and found in astrophysical situations (for example, in the solar corona), measurements of the ratio of intensities of lines radiated from two excited states of the same ion species, or of lines radiated by excited ions of the same species in different charge states can provide a sensitive measure of plasma electron temperature, if the relevant excitation and ionization cross sections are known. The "effective Gaunt factor" predictor formula or $\bar{g}$ approximation[5,6] proposed by Seaton relates the collision strength to the oscillator strength for the transition and has been widely employed to estimate excitation cross sections. Its reliability, however, cannot be expected in general to be better than a factor of 2, so that accurate experimental and theoretical cross sections are seriously needed.

Ions of the lithium isoelectronic sequence are particularly suitable candidates for detailed theoretical and experimental study. Energy levels

for Li-like Be^+, C^{3+}, and N^{4+} are indicated in units of the $2s$-$2p$ excitation energy in Fig. 1. The $2s$-$2p$ resonance lines are strong and readily observable in plasmas; thus a significant number of rate coefficients measured in plasmas have involved this transition in various ions.[7,8] In addition, since Li-like ions have only three electrons, and only one active valence electron, and since the $2s$ and $2p$ levels are well removed from other states, they present an optimal system for the testing of various theoretical methods and scaling models. In addition, Li-like ions possess no long-lived metastable states so that a ground-state target ion beam can be assured experimentally.

Considerable theoretical activity has been focused specifically on the lithium isoelectronic sequence, which has served as a useful testing ground for various computational methods. Calculations have
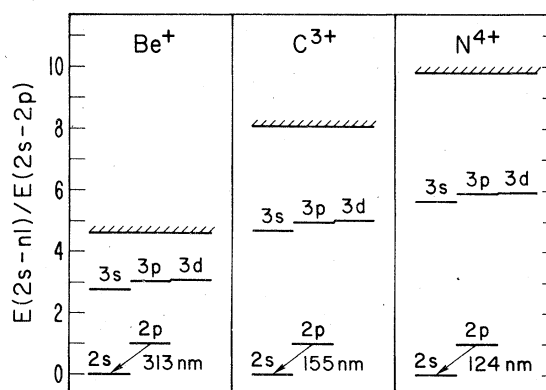

FIG. 1. Energy levels for the lithium like ions, Be^+, C^{3+}, and N^{4+}, scaled in units of the $2s$-$2p$ excitation energy.

utilized a wide range of approximations, which include the use of Coulomb wave functions in the Born, Bethe, and distorted-wave approximations, as well as more sophisticated close-coupling formulations that evaluate the roles of up to five atomic states in the collision. For the first ionic member of the sequence, Be$^+$, unpublished[9] but often quoted[10-12] experimental results of Taylor et al. lie approximately 18% below the most elaborate five-state close-coupling calculations.[10,11] This discrepancy lies outside the total estimated experimental uncertainty ($\pm$8%). Furthermore, an optical recalibration of the experiment against a second radiometric standard has just been completed, confirming the earlier calibration. In this case the role of other levels in the excitation process is significant, as evidenced by the fact that near threshold the first (CBXI) and second (CBXII) Coulomb-Born approximations (including exchange) are, respectively, factors of 1.96 and 1.23 larger than the five-state close-coupling calculation (5CCX). The inclusion of additional states beyond 5CCX in the close-coupling calculations is not expected to alter the results significantly.[11]

As the nuclear charge increases along the isoelectronic sequence, the effects on scattering of coupling to other levels is expected to diminish, since the energy of the $2p$ level varies as $Z + 1$, while the energies of higher n levels vary roughly as $(Z + 1)^{1.8}$. This progression of energy levels for Be$^+$, C^{3+}, and N^{4+} is shown in Fig. 1. Indeed, this expectation was substantiated in the case of C^{3+}, where Coulomb-Born (CBXI)[13] and close-coupling (2CCX,[13] 5CCX[14]) calculations agree within 6% at the 8-eV threshold energy and are also in agreement with recent absolute experimental data.[15]

Excitation of the $2s$-$2p$ transition in N^{4+} has also been the focus of considerable theoretical activity, some of the results of which are presented in Fig. 2. The various computational methods span the range from the classical binary-encounter approximation (BEA[16]) through quantum-mechanical Coulomb-Born (CB)[17-21] and Coulomb-distorted-wave (CDW)[22] formulations, to two-state (2CC)[17,19] and five-state (5CC)[17,19,23] close-coupling calculations. The effect of exchange has been evaluated in some of the close-coupling calculations[17,19] and was found to reduce the computed cross sections by about 6% at the lowest energies, with less effect at higher energies. Indeed, over the entire energy range from the 10 eV threshold to 300 eV, the largest difference between any of the quantum-mechanical calculations is only (8–10)%, indicating a relative insensitivity to the approximation used. It has also been shown[20] that plane-wave Born and Coulomb-Born results converge to better
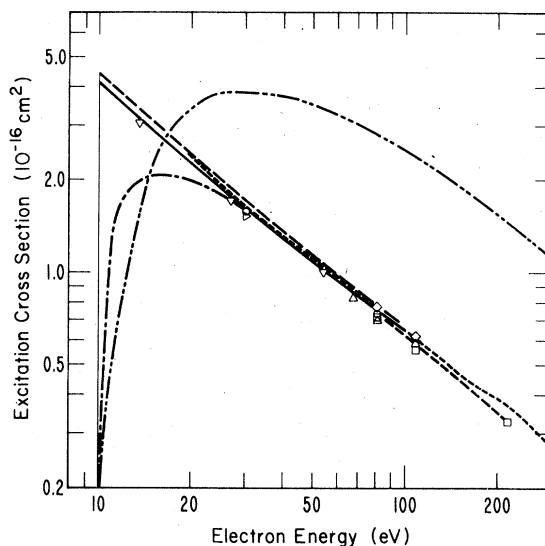

FIG. 2. Theoretical cross sections for $1s^2 2s$-$1s^2 2p$ excitation of N^{4+} by electron impact. Long dashes, CBI (Ref. 18); medium dashes, CBI (Ref. 17); short dashes, CBII (Ref. 19); solid curve, CBII (Ref. 18); ———·———, plane-wave Born approximation (PWBA) (Ref. 20); ———··———, classical (Ref. 16); O, CDW (Ref. 21); ▷, 2CCX (Ref. 17); ∇, 2CCX (Ref. 19); ◇, 5CCNX (Ref. 17); △, 5CCX (Ref. 22); □, 5CCX (Ref. 19).

than 10% for $2s$-$2p$ excitation of N^{4+} above 30 eV. The plane-wave Born and the classical binary-encounter approximations are incapable of accounting for the finite cross section at threshold, which is a characteristic of ion excitation. The classical calculation also overestimates the quantum results by a factor of 4 at 200 eV. The effective Gaunt factor, or $\bar{g}$ approximation, with $\bar{g}$ values tabulated by Van Regemorter[6] has proven quite reliable in general for singly charged positive ions[24]; however, for N^{4+}, predicted cross sections fall roughly a factor of 4 below the quantum results. It has been noted earlier by Bely[18] that these values for $\bar{g}$ are inappropriate for $2s$-$2p$ transitions in Li-like ions and are probably too small for multiply charged ions in general.

Cross section measurements of electron-impact excitation of ions have almost exclusively dealt with singly charged ions, and of these only a relatively small number of absolute experiments have been completed. Experimental and theoretical methods and results have been reviewed in articles by Dolder and Peart[25] and by Seaton,[26] respectively. Measurements on multiply charged ions include cross sections for 479.7 nm emission[27] from Hg^{2+} and a preliminary report by Bradbury et al.[28] on $2s$-$2p$ excitation of N^{4+}. Final results from the latter experiment have not been published, and extremely low signal levels in the

former did not permit precise cross sections to be determined. The cross section measurements for C^{3+} $2s$-$2p$ excitation, which have been reported in a recent Letter,[15] are considered to be the first definitive experimental results for electron excitation of a multiply charged ion. The present measurements on excitation of N^{4+} provide a further test of the theoretical excitation cross sections for multicharged lithiumlike ions. A discussion of the experimental techniques and uncertainties is presented, and new absolute results for excitation of N^{4+} are reported for electron energies ranging from below the 10 eV threshold to 52 eV. The experimental cross sections for N^{4+} are compared with available theoretical calculations and correlated with similar comparisons for C^{3+}. Rate coefficients have been deduced from the data for comparison with plasma measurements.

II. EXPERIMENTAL

A. General method

The crossed-beams technique for measurement of ion excitation cross sections has been discussed in detail in previous reports.[29,30] A schematic of the apparatus used for the present N^{4+} excitation measurements is shown in Fig. 3. A collimated and mass-to-charge analyzed beam of N^{4+} ions collides at right angles with a magnetically confined beam of variable energy electrons, and the flux of photons emitted by excited ions into a known solid angle normal to their plane of intersection was detected by a vacuum-ultraviolet (vuv) photomultiplier and counted. Absolute calibration of the photodetector response at the wavelength of interest was achieved by utilization of a well-defined photon collection geometry and by comparison of the photodetector sensitivity to that

of a standard U. S. Natl. Bur. Stand. calibrated photodiode. The experiment was performed in a region of ultrahigh vacuum ($<10^{-7}$ Pa or 8×10^{-10} Torr) to minimize the number of photons produced by beam collisions with residual gas. Background events were separated from the much smaller electron-ion excitation signal by chopping both ion and electron beams and gating the photon counters appropriately. An on-line computer was utilized to control the experiment and to register and reduce the data. The cross sections for excitation may be related to measured parameters according to the usual relationship,[29]

$$\sigma = \frac{Rqe^2}{I_i I_e} \frac{v_i v_e}{(v_i^2 + v_e^2)^{1/2}} \frac{\mathcal{F}}{Y_\Omega D(Z_0, \lambda)}, \quad (1)$$

where R is the measured photon count rate; I_i and I_e are the ion and electron currents; qe is the ionic charge; v_i and v_e are the ion and electron velocities; Y_Ω accounts for any anisotropy in the emitted radiation; and $\mathcal{F}$ is the form factor which accounts for the spatial overlap of the beams, for any spatial variations in the detection efficiency of the photodetector, and for the fact that the excited ions have a finite lifetime. $D(z_0, \lambda)$ is the absolute average probability that a photon of wavelength λ emitted isotropically from the $z = z_0$ plane in the center of the beam intersection volume will be detected. The experiments were performed by making an absolute cross section measurement at one electron energy just above threshold with the photon collection geometry well characterized. Due to the extremely low signal count rates, measurements at other electron energies were made with a hollow reflective light guide inserted between the interaction volume and the photodetector to increase the effective photon collection solid angle. These relative cross section data were then normalized to the one absolute cross sec-
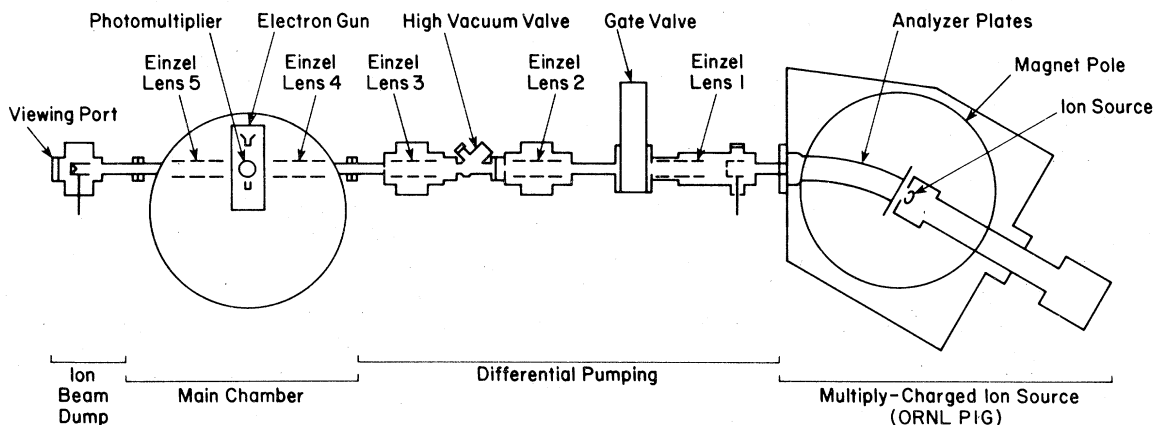

FIG. 3. Schematic diagram of the apparatus.

tion measurement. Uncertainty introduced due to anisotropy of the radiation is discussed in Sec. IID.

B. Ion beam

The N^{4+} ions at 39 keV were extracted from the Oak Ridge cold cathode Penning discharge source (ORNL PIG),[31] with acceleration transverse to the magnetic field. A pair of curved plates produces an electrostatic field transverse to the magnetic field and permits ions of a particular mass-to-charge ratio (m/q) to be directed through an exit aperture placed outside the magnetic field.

The majority of the C^{3+} excitation measurements reported previously[15] were made using a system which was designed to facilitate measurement of cross sections for electron-impact ionization as well. This transport system provided electrostatic charge purification just prior to, and analysis just downstream of, the beam intersection volume and has been described in detail in a recent report on C^{3+} and N^{4+} ionization cross section measurements.[32] To compensate somewhat for the lower N^{4+} ion flux from the source, reduced photodetector sensitivity and increased background levels, a new ion-beam transport was designed for the N^{4+} excitation experiment which allowed a larger fraction of the ion-source output to be directed through the beam interaction volume. This system is shown schematically in Fig. 3. No specific provision was made in this system for removing unwanted charge states from the target beam (primarily N^{3+} formed by electron capture on residual gas) just before the beams intersect, but the combination of high vacuum in most of the beam transport system and the rejection of ions of incorrect energy per unit charge (E/q) by the relatively strong focusing lenses ensured an N^{4+} target beam of high purity. Subsequent experiments using this system have demonstrated that the N^{4+} beam contains less than 1% of ions in other charge states. Three differentially pumped chambers containing Einzel lenses and deflector plates are separated by 6.4-mm-diam circular apertures located near the crossovers of the lenses. Two more sets of Einzel lenses and deflectors in the main chamber focus the beam into the collision chamber and subsequently into the final Faraday cup, which is housed in a separately pumped chamber in order to minimize vacuum loading by the ion beam. The ion beam can be completely switched off by applying voltage to the deflector plates of the first two Einzel lenses.

An aperture located 4.5 cm upstream from the center of the collision volume is the limiting ion-beam aperture in the horizontal direction. Proper focusing and deflection by Einzel 4 allows the ion beam to pass through this aperture and the entrance and exit apertures of the collision chamber without significant current loss or creation of excessive photon noise at the photomultiplier. The Einzel 4 vertical deflector plates are used to position the beam at the collision volume. Since the charged ion beam passes through the collision volume perpendicular to the electron-confining magnetic field, the resulting Lorentz force changes the beam direction slightly. Vertical deflector plates on either end of the collision volume compensate for this effect. The differential current distributions of the ion and electron beams in the vertical direction were recorded at their point of intersection by means of an externally driven slit 0.2 mm high and 6 mm wide, which could be rotated to intercept either beam. The beam at the position of intersection with electrons was about 0.3 cm high by 0.2 cm wide, and typical ion-beam currents in the collision volume ranged from 1–2 μA for N^{4+} and 4–6 μA for C^{3+}. Using the earlier beam transport system,[32] C^{3+} beam currents of 0.5 μA were typical. The ion-beam energy is deduced from the accelerating voltage, and due to the possible plasma potential, may be uncertain by up to 100 V or 1%.

C. Electron beam

In order to provide measurable excitation signals near threshold in a crossed-beams experiment, an electron source is needed which is capable of producing high-intensity beams (10–100 μA) at low energies (<10 eV for N^{4+}). A magnetically confined electron gun similar to that developed and thoroughly characterized by Taylor et al.[33] was utilized in the present experiments. The indirectly heated planar oxide-coated cathode was located 5 cm from the scattering volume. A series of eight electrodes containing apertures was spaced at intervals along the beam path. The aperture dimensions were chosen to minimize the electron current hitting surfaces within the field of view of the photodetector. The electrodes were held at negative potentials in linear proportion to their distance from the collision cell anode. Such an arrangement imparts minimal transverse energy to the electrons and thus minimizes spiraling about the axial magnetic field lines.[33] The beam was gated off by making the potential on one of the electrodes more negative than the cathode. The electron beam was about 0.7 cm tall and 0.2 cm wide in the collision volume. Since the ion beam was contained within the electron beam the form factor $\mathcal{F}$ in Eq. (1) was thus about 0.7 cm. For the present experiments a special collector

was designed to minimize the number of reflected electrons, which because of the axial magnetic field (0.02 T) are likely to travel back through the collision volume. Details of the design and performance of this collector are given in another report.[32] Measurements of currents to other electrodes indicated that about 1% of the incident electron beam was reflected back through the collision volume at 100 eV, and an appropriate uncertainty has been allowed in the collected electron current. Secondary electrons ejected from the collector totaled 3% of the measured current and were easily held by the application of a positive bias of 50 V or more. Currents to other electrodes located downstream of the collision volume were negligible.

The actual electron-beam energy in the collision volume differed from the voltage applied to the cathode due to the effects of thermal kinetic energy from the cathode, beam space charge, surface contact potentials, and the penetration of fields applied to compensate for the deflection of the ion beam by the electron-confining magnetic field. These effects are particularly important at the lower energies near threshold and result in a shift and distribution broadening of electron energies in the beam. Corrections to the energy for the effects of space-charge depression and to the effective path length due to spiraling about the magnetic field lines were made using empirical formulas determined during previous experiments with a similar electron gun.[29,33] In the present experiments there was a further energy shift (about 1 eV) and spread due to field penetration from the ion deflector plates. Since surface contact potentials could not be directly measured, the actual energy calibration and determination of the energy distribution were made using the known thresholds for ($2s$-$2p$) excitation of C^{3+} (8.0 eV) and N^{4+} (10.0 eV), and the fact that cross sections for ion excitation are in general characterized by an infinite slope at threshold. The energy distribution determined in this manner can be represented by a Gaussian with a full width at half maximum (FWHM) of 2.9 eV and is consistent with estimates of the contributions of the various sources listed. The contact potential of 2 V was consistent with previously determined values for similar oxide-coated cathodes.[33]

D. Photon flux measurement

The absolute cross section for $2s$-$2p$ excitation of N^{4+} at 15.5 eV was determined by detecting the photon flux into a well-defined $f/3$ aperture using a solar-blind photomultiplier whose quantum efficiency at 124 nm was measured immediately following the measurements by direct comparison to a standard vuv photodiode[34] calibrated by the U. S. Natl. Bur. Stand. There are no other spectral lines of N^{4+} at wavelengths within the sensitivity range of the detector used.

In the photomultiplier (PMT) quantum efficiency measurements, 124 mm light from a gas discharge lamp was selected by a grating monochromator and was alternately transferred between the standard diode and the PMT by means of a rotatable mirror. The movable mirror was also used to scan a small light spot over the surface of the PMT, so that variations in sensitivity could be taken into account. In the crossed-beams apparatus, the PMT is housed in a magnetic shield and supported from the electron gun assembly. The approximately 8 W dissipated by the electron filament cause the PMT to operate in vacuum at a temperature of 77 °C, as determined by an attached thermocouple. The quantum efficiency measurements were thus carried out with the PMT heated to several temperatures ranging from 20 to 70 °C. At 124 nm the PMT became more sensitive with increasing temperature at the rate of 0.22% of the quantum efficiency per °C. The measured quantum efficiency under operating conditions at 124 nm was 0.095.

The pulse transmission (ratio of events counted to total number of events) depends on the gain of the PMT as well as that of the electronics for a given pulse amplitude discriminator setting and was monitored regularly during both cross section and quantum efficiency measurements. For the photomultiplier employed here[35] with linear pulse amplification, integral pulse-height distributions, plotted as logarithm of count rate versus discriminator setting, are linear over a wide pulse-height range, and extrapolation to zero pulse height was taken to represent the total number of events. It is noted that the exponential character of the pulse-height distribution may not extend to zero pulse height for some PMT's,[36] although no such departures were found for the present detector. Pulse transmissions during calibration and cross section measurements were made comparable, so that the fraction of photons detected was nearly the same in each case, minimizing possible effects on the measurements. A small uncertainty has been allowed to account for the variations in pulse transmission (62%–78%) during the measurements. Corrections for system dead time were negligible for the count rates encountered in the cross section measurements but were taken into account in the quantum efficiency calibration.

The solid angle subtended by the photodetector at the collision volume was determined for ab-

solute measurements by purely geometrical considerations. No windows or lenses were used, and the solid angle was defined by a 2.54-cm-diam aperture placed immediately in front of the PMT face, 7.6 cm from the center of the beam collision volume. The collision chamber and surfaces visible to the PMT were coated with gold black to minimize any reflections. The absolute probability $D(z, \lambda)$ that a photon of wavelength λ emitted isotropically from a point of vertical position z would be registered as an event was evaluated by calculating the solid angle subtended at various heights z in the collision volume by a surface element of the photocathode, multiplying by the measured quantum efficiency of that element, and numerically integrating over the active photocathode are defined by the limiting aperture. The value of $D(z_0, x)$ in this experiment was approximately 4×10^{-4}.

The calibration procedure outlined above assumes that photons produced by the interaction of the beams are radiated isotropically in space. However, ions excited by electron impact may radiate anisotropically. This anisotropy is expressed in terms of the light polarization P and the angle between the electron beam and the detector, θ, as

$$Y_\Omega = (1 - P\cos^2\theta)/(1 - \tfrac{1}{3}P). \qquad (2)$$

In the present experiments, measurement of the polarization was not practical, and theoretical values of the polarization calculated as functions of electron energy by Gau and Henry[14] were used in Eq. (2) to correct the measured photon flux emitted at angle θ for anisotropy of the radiation. Values of Y_Ω ranged from 1.021 to 1.007.

Account must also be taken of the fact that the excited states of the moving ions have finite lifetimes ($\tau = 3$ nsec for N^{4+} and 4 nsec for C^{3+}), and consequently some fraction of the ions excited by electron impact will radiate downstream beyond the field of view of the detector, or at some point from which the probability of detection is reduced. Since the excited state lifetime (τ) and ion velocity (v_i) are known, this effect can be readily evaluated. The characteristic decay length $v_i\tau$ is 0.22 cm for the present experiment, and evaluation of this effect results in a 2.9% correction. For the absolute cross section measurement, the effects due to spatial variations in the PMT quantum efficiency, anisotropy due to polarization, excited ion lifetime, and variation of detection solid angle and beam current distribution with height z were evaluated by a simultaneous numerical integration procedure. The variation of detection efficiency over the width of the beam (0.2 cm) was negligibly

small and was ignored in the integrations.

Due to extremely low signal count rates encountered in the absolute cross section measurements, a hollow aluminized cylindrical quartz light guide was inserted between the collision volume and the PMT face in order to increase the effective photon collection solid angle for measurements at other electron energies. The aluminized surface was overcoated with MgF_2 in order to increase reflectivity at 124 nm. These measures increased the effective solid angle accepted by the detector by roughly a factor of 3. Due to the uncertainties involved in determining the reflectivity of the light guide and thus the effective solid angle for detection, absolute measurements were not attempted with the light guide in place. Relative data were obtained over a range of electron energies under these conditions and were then normalized to the absolute measurement at 15.5 eV. The only energy-dependent quantity which is affected by this increase in effective solid angle, is the anisotropy correction factor [Eq. (2)]. Assuming $\theta = 90°$ (i.e., maximum anisotropy effect), the total correction to the data at 52 eV relative to that at 10 eV is only 1%, so that the uncertainty in θ contributes less than 1% to the uncertainty in the relative cross section.

E. Cross-section measurements and uncertainties

The most difficult problem encountered in crossed-beam experiments generally is the separation of beam-beam events from those produced by interactions of either beam with residual gas or surfaces. In the present apparatus the beam apertures were arranged to minimize electrons or ions hitting surfaces within the field of view of the detector, and pressure in the collision region was kept below 1.3×10^{-7} Pa ($\sim 1 \times 10^{-9}$ Torr) by a combination of titanium sublimation and ion pumping. The primary ion beam was also collected in a separate differentially pumped chamber in order to minimize ion beam loading of the vacuum in the collision chamber. Despite these precautions, background photon count rates exceeded the electron-ion signals by as much as three orders of magnitude at the higher electron energies. For example, for a 52-eV electron beam of about 250 μA crossing at 1 μA beam of N^{4+} ions in a vacuum of 1×10^{-7} Pa, a signal of 0.6 sec^{-1} was obtained against a background of 700 sec^{-1}. Under these conditions, 54 h of data acquisition time were required in order to obtain a measurement with a standard deviation of the mean of 10%.

In order to separate the electron-ion excitation signals from the much larger photon backgrounds, an on-line computer was programmed to generate

a series of switching signals which were used to chop both the electron and ion beams, and to gate two scalers which counted the photomultiplier pulses. The scheme was based on that used by Dance et al.[37] and by Harrison,[38] and included provision for averaging any irregularities across the beam current pulses, between scalers, and for inhibiting the scalers from counting while beams were switching. A modulation frequency of 0.5 kHz was used for the measurements, and was selected such that the period was much smaller than the pumping time constant of the vacuum system. Under these conditions, the likelihood of generation of noncancelling background signals due to beam modulation of the background gas pressure is minimized.

Systematic tests were performed to verify that the apparent cross section for excitation was indeed zero below the 10 eV $2s$-$2p$ threshold, and also to investigate any possible spurious dependence of the measured cross sections on the beam intensities. A decrease of the apparent cross section with increasing electron current was observed at the highest electron energy (52 eV);

thus the "true" cross section at this energy was obtained by a linear extrapolation of the measured apparent cross section to zero electron current. A discussion of this effect is given in the Appendix. Analysis of the data taken at 52 eV for a possible dependence of the apparent cross section on ion current failed to reveal a spurious dependence that was significant at the one standard deviation level for ion currents varying by almost a factor of 3.

In Table I, the estimated sources of experimental uncertainty in both the relative cross section measurements and the absolute radiometric calibration are listed. The individual uncertainties associated with systematic effects were evaluated at a "good" confidence level, believed to be equivalent to the 90% confidence level (CL) on counting statistics. Uncorrelated systematic uncertainties were combined in quadrature to given the total uncertainty in the relative cross section measurements, in the absolute optical calibration, and finally the total systematic experimental uncertainty (18%) at good confidence level. The total absolute uncertainty for individual data points was

TABLE I. Experimental uncertainties.[a]

	10 eV (%)	52 eV (%)
A. Crossed-beams measurement		
Anisotropy correction factor	2.0	0.5
Beam overlap factor	3.0	3.0
Path length	2.0	0.5
Uncollected ions	0.5	0.5
Uncollected electrons	0.5	1.0
Electron current measurement	2.0	2.0
Ion current measurement	2.0	2.0
Ion velocity	1.0	1.0
Lifetime correction	0.5	0.5
Spurious electron current dependence	2.0	7.0
Photon counting efficiency	5.0	5.0
Quadrature sum	7.5	9.7
B. Absolute radiometric calibration		
Uncertainty in NBS-calibrated photodiode	15.0	
Transfer statistics	3.0	
Temperature dependence of quantum efficiency	2.0	
Determination of effective solid angle	2.0	
Spatial variations of sensitivity	2.0	
Photocurrent measurement and counting efficiency	2.0	
Quadrature sum	15.8	
C. Total uncertainties		
Quadrature sum	17.5	18.5

[a]Uncertainties have been estimated at "good" confidence level, believed equivalent to 90% CL on statistical uncertainties.

taken to be a quadrature sum of the total systematic uncertainty and the 90% CL random uncertainty.

F. Experimental results

Absolute experimental cross sections for $1s^2 2s$-$1s^2 2p$ excitation of N^{4+} by electron impact are plotted in Fig. 4. As discussed earlier in Sec. II E, the solid point at 15.5 eV represents an absolute cross section measurement, and relative measurements of the excitation function at other energies (open points) were normalized to this value. The error bars represent the random uncertainty at 90% confidence level, and the other bars on the absolute point represent the estimated total experimental uncertainty at good confidence level, including that of the absolute radiometric calibration. The dashed curve represents the two-state close-coupling calculation with exchange of Van Wyngaarden and Henry,[19] which is representative of the quantum calculations. A convolution of this theoretical curve with the estimated experimental electron energy distribution (represented by a Gaussian with a FWHM of 2.9 eV) gives the solid curve which, if the theory is correct, represents what would be expected of a measurement using our electron beam. The excellent agreement between theory and experiment may be
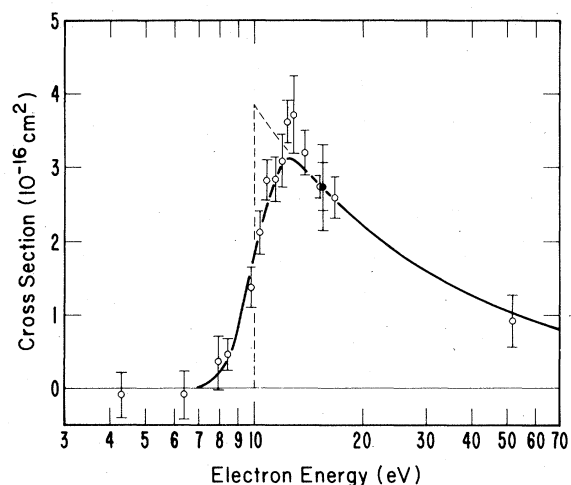

FIG. 4. Absolute cross section vs electron energy for $2s$-$2p$ excitation of N^{4+} by electron impact. Solid point at 15.5 eV represents an absolute measurement, relative to which open points at other energies were measured. Dashed curve represents two-state close coupling with exchange calculation (2CCX) from Ref. 19, and solid curve is a convolution of the experimental electron energy distribution with the dashed curve. Bars on experimental points designate random uncertainties at 90% confidence level, and outer bars on solid point represent the total experimental uncertainty at good confidence level (see Table I and text).

considered somewhat fortuitous, considering the magnitude of the absolute experimental uncertainty ($\pm 18\%$). The latter is dominated by the $\pm 15\%$ (good confidence level) uncertainty in the U. S. Natl. Bur. Stand. calibrated standard photodiode, and it is suspected that this uncertainty given by the U. S. Natl. Bur. Stand. is extremely conservative, especially since a similar level of agreement was obtained in the case of C^{3+} excitation using the same standard. The present experimental data represent the $2s$-$2p$ excitation cross section only, since the threshold energies for contributions to the 124 nm emission due to cascade from the higher $3s$ and $3d$ levels occur at 59.2 and 60.0 eV, above the highest measurement at 52 eV. In addition, there are no other transitions of N^{4+} that lie within the sensitivity bandwidth of the photon detector.

As noted in Sec. I, all the quantum-mechanical calculations for $2s$-$2p$ excitation of N^{4+} are in agreement to within 10% or better, so the uncertainty in the experimental results does not permit a relative evaluation of the theoretical methods. Published experimental[15] and theoretical[13] results for $2s$-$2p$ excitation of C^{3+} are presented in Fig. 5 for comparison, and the experimental data for both C^{3+} and N^{4+} excitation are collected in Table II. Data are tabulated only for those electron energies for which the experimental electron energy spread does not significantly affect the measurements (i.e., >10 eV for C^{3+} and >12 eV for N^{4+}). The level of agreement between the theories and experiment is comparable in the C^{3+} case. The results for C^{3+} and N^{4+} suggest that electron-impact excitation of the higher-Z members of the lithium isoelectronic sequence can be reliably characterized (at least to the $\pm 18\%$ level) by any of the quantum-theoretical approximations which have been employed, and that the insensitivity to the particular approximation used stems from the increasing isolation of the $2s$ and $2p$ levels relative to other states as Z increases. This simplification suggests that measurement of the photon emission from Li-like ions should be a particularly reliable diagnostic for analysis of high-temperature plasmas.

In Fig. 6 are plotted Maxwellian rate coefficients for N^{4+} excitation deduced from the close-coupling calculations of Van Wyngaarden and Henry[19] (which adequately represent the present experimental data). Also plotted are experimental plasma rate coefficient measurements by Boland et al.[7] and by Kunze and Johnson[8] in the 10–300-eV temperature range. The similar agreement within experimental uncertainties between the theoretically deduced rate coefficients and the experimental rate measurements is taken as evidence
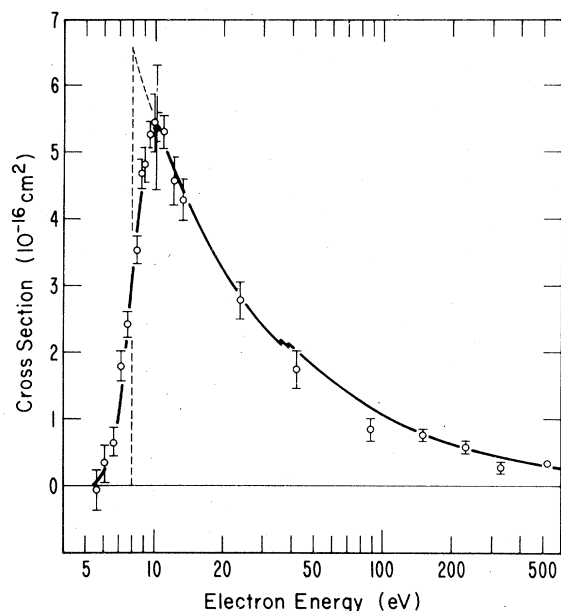
FIG. 5. Absolute cross section vs electron energy for emission of $2p$-$2s$ radiation (155 nm) by electron impact on ground state C^{3+} ions. The experimental data are taken from Ref. 15. Solid point at 10.2 eV is an absolute measurement, relative to which open points at other energies were measured. Dashed curve represents two-state close-coupling calculation with exchange (2CCX) from Ref. 13, including estimates of the $2s$-$3s$ and $2s$-$3d$ cascade contributions. Solid curve is a convolution of the experimental electron energy distribution with the dashed curve. Bars represent random uncertainties at 90% confidence level, and outer bars on solid point designate total experimental uncertainty at good confidence level.

TABLE II. Experimental cross section data.

Electron energy (eV)	Cross section[a] (10^{-16} cm^2)
N^{4+}	
12.4	3.66 ± 0.30
13.0	3.75 ± 0.53
13.9	3.23 ± 0.30
15.5	2.74 ± 0.33
16.8	2.62 ± 0.28
52.1	0.86 ± 0.33
C^{3+}	
10.5	5.31 ± 0.24
11.1	4.57 ± 0.36
13.3	4.29 ± 0.30
22.7	2.77 ± 0.27
42.1	1.74 ± 0.27
89.6	0.84 ± 0.16
151.3	0.76 ± 0.07
233.1	0.57 ± 0.08
329.8	0.28 ± 0.06
530.8	0.32 ± 0.02

[a] Error limits represent 90% CL random uncertainties. Total absolute systematic uncertainties at comparable confidence level are ±18% for N^{4+} and ±17% for C^{3+}.

for the consistency of the rate-coefficient and cross section measurements.

APPENDIX

In any crossed-beams experiment, it is necessary to demonstrate that the measured cross sec-
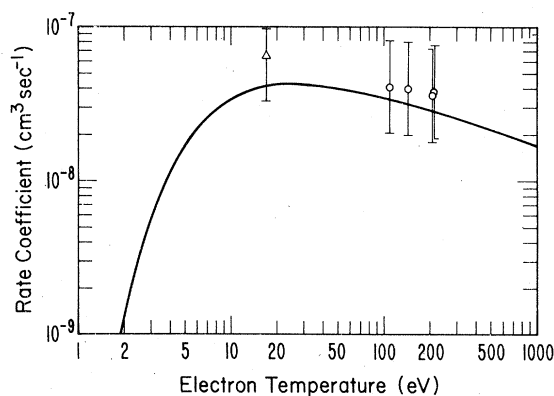

FIG. 6. Rate coefficients vs Maxwellian electron temperature for $2s$-$2p$ excitation of N^{4+} by electron impact. Curve is computed from two-state close-coupling calculation of van Wyngaarden and Henry (Ref. 19), which is consistent with the present experimental cross section data extending from 10 to 52 eV. Circles and triangles are, respectively, the plasma excitation rate coefficient measurements of Kunze and Johnston (Ref. 7) and of Boland et al., (Ref. 8).

tions do not depend on the intensities of the beams. Under some circumstances, the mutual space-charge interaction between the charged beams can cause one beam to focus or deflect the other in such a way that a change in noise may be observed when both beams are on.[38] In the present experiment, the current density of the electron beam was typically 5 times that of the ion beam, and such an effect, if present, might be expected to produce a spurious signal at electron energies below the 2s-2p excitation threshold, and/or possibly an electron-density-dependent "cross section" at higher energies. Similarly, spurious signals may arise from any two-step process involving excitation of background gas for which both beams are required to either produce the relevant state of excitation (whose decay results in detectable light), or to cause the excited state to be quenched in some manner. As may be seen from Fig. 4, no statistically significant cross section was measured at energies below the N^{4+} excitation threshold (4.3 and 6.4 eV).

The measured dependences of the apparent cross section on electron current at electron energies of 16.8 and 52 eV are shown in Fig. 7. The poor signal-to-noise ratios and low signals limited the statistical precision of these measurements, but one may reasonably conclude that a current dependence is either absent, or small at 16.8 eV, but is significant at 52 eV. The solid points at 52 eV were taken with the height of the electron beam defining aperture reduced by $\frac{1}{3}$, and are
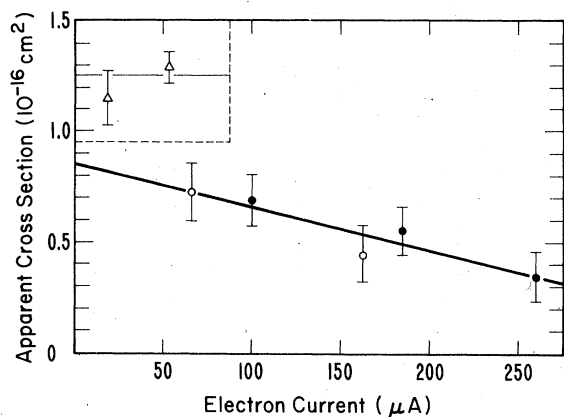
consistent with the remaining data (open points). This is taken as evidence that the process which gives rise to spurious cross section is dependent upon electron current rather than electron density, and thus is more likely produced by interactions of the beams with residual gas than by a surface effect caused by steering or focusing of the ion beam by the electron beam. Additional evidence for this hypothesis derives from the fact that the spurious effect does not appear at energies at or below 16.8 eV, despite the fact that the density of the electron beam changes by less than 60% between 4 and 52 eV. The nature of the source of the spurious electron current dependence is not understood, nor is the reason for its presence in the N^{4+} measurements, and not in the C^{3+} data.[15] It is suspected that the detector sensitivity to shorter wavelengths in the N^{4+} experiments may be responsible, since the background photon fluxes were substantially larger than in the C^{3+} case. The data in Fig. 7 at 52 eV are consistent with a linear dependence of apparent cross section on electron current, and the line shown represents a linear least-squares fit to the data. The zero-current intercept is taken as the true cross section at this energy.
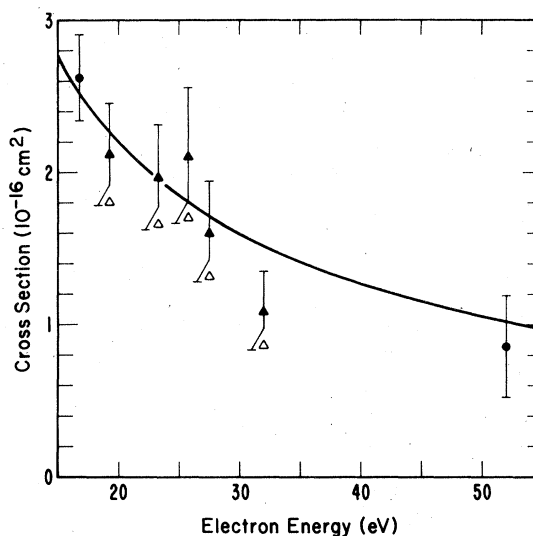

FIG. 7. Apparent cross section vs electron current for 2s-2p excitation of N^{4+} at electron energies of 16.8 eV (triangles) and 52.0 eV (circles). The cross sections at 16.8 eV have been divided by 2 to facilitate plotting. Solid points were taken with the electron beam current density increased by a factor of 1.5 (see the Appendix). The straight line at 52 eV represents a linear least-squares fit to the data. Bars are one standard deviation statistical only.

FIG. 8. Experimental cross sections vs electron energy for 2s-2p excitation of N^{4+} in the 16–52-eV region. Solid circles at 16.8 and 52.0 eV represent data from Fig. 4. Additional points (open triangles) represent additional data for which corrections for a likely spurious dependence on electron current were not measured. Solid triangles represent open data points corrected using the same current-dependent correction as was measured at 52 eV (see the Appendix). Bars are random uncertainties at 90% confidence level. The solid curve is the close-coupling calculation (2CCX) of van Wyngaarden and Henry (Ref. 19).

In addition to the data shown on Fig. 4, cross section measurements were made at five additional energies between 19 and 32 eV. Due to the low signal level and signal-to-noise ratios, it was not judged practical to measure electron current dependences at these energies. As a result these data were judged to be uncertain and are not presented on Fig. 4. It is possible however to estimate corrections to these data points for a possible electron current dependence based on the measurements made at other energies. The absence of a significant cross section below threshold and of a current dependence at 16.8 eV suggests that the spurious process responsible for the effect at 52 eV has a threshold energy somewhere between these two energies. Since the data of Fig. 7 at 52 eV suggest a linear dependence of the correction factor on electron current, the assumption was made that the correction at all energies above 18 eV had the same current dependence as that measured at 52 eV, and the curve in Fig. 7 was used to deduce relevant corrections factors for each datum point. In Fig. 8, the raw and corrected data between 19 and 32 eV are plotted, along with the theoretical curve and the secure data at 16.8 and 52 eV from Fig. 4. Such a correction procedure brings these measurements into reasonable agreement with the theory, and makes them consistent with the remainder of the data.

---

*Present address: Brookhaven National Laboratory, Upton, N.Y.

†Staff member: Quantum Physics Division, National Bureau of Standards.

[1] L. Heroux, Proc. R. Soc. 83, 121 (1966).

[2] J. T. Hogan and H. C. Howe, J. Nucl. Mater. 63, 151 (1976).

[3] R. V. Jensen, D. E. Post, W. H. Grasberger, C. B. Tarter, and W. A. Lokke, Nucl. Fusion 17, 1187 (1977); At. Data 20, 397 (1977).

[4] R. C. Isler, R. V. Neidigh, and R. D. Cowan, Phys. Lett. A 63, 295 (1977).

[5] M. J. Seaton, in Atomic and Molecular Processes, edited by D. R. Bates (Academic, New York, 1962), p. 416.

[6] H. van Regemorter, Astrophys. J. 136, 906 (1962).

[7] B. C. Boland, R. C. Jahoda, T. L. Jones and R. W. P. McWhirter, J. Phys. B 3, 1134 (1970).

[8] H.-J. Kunze and D. W. Johnson, Phys. Rev. A 3, 1384 (1971).

[9] P. O. Taylor, R. A. Phaneuf, and G. H. Dunn (private communication).

[10] M. A. Hayes, D. W. Norcross, J. B. Mann, and W. D. Robb, J. Phys. B 10, L429 (1977).

[11] R. J. W. Henry and W.-L. van Wyngaarden, Phys. Rev. A 16, 986 (1977).

[12] J. V. Kennedy, V. P. Myerscough, and M. R. C. McDowell, J. Phys. B 11, 1303 (1978).

[13] N. H. Magee, Jr., J. B. Mann, A. L. Merts, and W. D. Robb, Los Alamos Scientific Laboratory Report No. LA-6691-MS, 1977 (unpublished).

[14] J. N. Gau and R. J. W. Henry, Phys. Rev. A 16, 986 (1977).

[15] P. O. Taylor, D. Gregory, G. D. Dunn, R. A. Phaneuf, and D. H. Crandall, Phys. Rev. Lett. 39, 1256 (1977).

[16] K. C. Mathur, A. N. Tripathi, and S. K. Joshi, Int. J. Mass. Spectrom. Ion Phys. 7, 167 (1971).

[17] P. G. Burke, J. H. Tait, and B. A. Lewis, Proc. Phys. Soc. 87, 209 (1966).

[18] O. Bely, Proc. Phys. Soc. 88, 587 (1966).

[19] W. L. van Wyngaarden and R. J. W. Henry, J. Phys. B 9, 146 (1976).

[20] J. A. Tully and D. Petrini, J. Phys. B 7, L231 (1974).

[21] M. Blaha, Astrophys. J. 157, 473 (1969).

[22] D. R. Flower, J. Phys. B 4, 697 (1971).

[23] M. A. Hayes, J. Phys. B 8, L8 (1975); and private communication.

[24] P. O. Taylor, R. A. Phaneuf, D. H. Crandall, and G. H. Dunn, in Electronic and Atomic Collisions, Abstract of Papers of the Ninth International Conference on the Physics of Electronic and Atomic Collisions, edited by J. S. Risley and R. Geballe (University of Washington, Seattle, 1975), p. 391.

[25] K. T. Dolder and B. Peart, Rep. Prog. Phys. 39, 693 (1976).

[26] M. J. Seaton, Adv. At. Mol. Phys. 11, 83 (1975).

[27] R. A. Phaneuf, P. O. Taylor, and G. H. Dunn, Phys. Rev. A 14, 2021 (1976).

[28] J. N. Bradbury, T. E. Sharp, B. Mass, and R. N. Varney, Nucl. Instrum. Methods 110, 75 (1973).

[29] P. O. Taylor and G. H. Dunn, Phys. Rev. A 8, 2304 (1973).

[30] P. O. Taylor, Ph.D. thesis, University of Colorado, 1973 (unpublished). (Available through University Microfilms, Ann Arbor, Mich.).

[31] M. L. Mallory and D. H. Crandall, IEEE Trans. Nucl. Sci. NS-23, 1069 (1976).

[32] D. H. Crandall, R. A. Phaneuf, and P. O. Taylor, Phys. Rev. A 18, 1911 (1978).

[33] P. O. Taylor, K. T. Dolder, W. E. Kauppila and G. H. Dunn, Rev. Sci. Instrum. 45, 538 (1974).

[34] L. R. Canfield, R. G. Johnston, and R. P. Madden, Appl. Opt. 12, 1611 (1973).

[35] EMR Model 542J. This is given for technical completeness, and is not intended to be an endorsement of this product.

[36] A. T. Young, Appl. Opt. 8, 2431 (1969); J. R. Prescott, Nucl. Instrum. Methods 39, 173 (1960); G. A. Morton, Appl. Opt. 7, 1 (1968).

[37] D. F. Dance, M. F. A. Harrison, and A. C. H. Smith, Proc. R. Soc. A 290, 74 (1966).

[38] M. F. A. Harrison, in Methods of Experimental Physics, edited by B. Bederson and W. L. Fite (Academic, New York, 1968), Vol. 7A, Chap. 1.4, pp. 95–115.